Optimal Boundary Control for Water Hammer Suppression in Fluid Transmission Pipelines [1]

Tehuan Chen[a], Zhigang Ren[a], Chao Xu[a2], Ryan Loxton[b]

[a] *State Key Laboratory of Industrial Control Technology and Institute of Cyber-Systems & Control, Zhejiang University, Hangzhou, Zhejiang 310027, China.*

[b] *Department of Mathematics & Statistics, Curtin University, Perth, Western Australia 6845, Australia.*

Abstract

When fluid flow in a pipeline is suddenly halted, a pressure surge or wave is created within the pipeline. This phenomenon, called water hammer, can cause major damage to pipelines, including pipeline ruptures. In this paper, we model the problem of mitigating water hammer during valve closure by an optimal boundary control problem involving a nonlinear hyperbolic PDE system that describes the fluid flow along the pipeline. The control variable in this system represents the valve boundary actuation implemented at the pipeline terminus. To solve the boundary control problem, we first use the method of lines to obtain a finite-dimensional ODE model based on the original PDE system. Then, for the boundary control design, we apply the control parameterization method to obtain an approximate optimal parameter selection problem that can be solved using nonlinear optimization techniques such as Sequential Quadratic Programming (SQP). We conclude the paper with simulation results demonstrating the capability of optimal boundary control to significantly reduce flow fluctuation.

Keywords: Water hammer, Optimal boundary control, Method of lines, Hyperbolic partial differential equation, Control parameterization method

1. Introduction

Water hammer occurs when fluid moving through a pipeline is forced to suddenly stop or change direction. This sudden change in motion, which could be due to valve closure, pump failure, or unexpected pipeline damage, causes a pressure wave to propagate along the pipeline at high speed [1, 2]. The wave speed can be over 1000m/s, with significant pressure oscillation, often causing loud noises and serious damage [3]. In severe cases, water hammer may even cause the pipeline to rupture, resulting in slurry and water leakage (examples of pipeline rupture are shown in Figure 1) [4]. Fluid pipeline failures due to water hammer effects are described in detail in [5, 6].

The mathematical equations describing water hammer consist of hyperbolic or parabolic partial differential equations. Numerous methods for solving these equations, and

[1] This work was partially supported by the National Natural Science Foundation of China through grants F030119-61104048, 2012AA041701 and 61320106009.

[2] Correspondence to: Chao Xu, Email: cxu@zju.edu.cn

Figure 1: Examples of pipeline damage caused by water hammer (Source: http://traction.armintl.com/traction#/single& proj=Docs&rec=403&brief=n)

thereby simulating water hammer, have been developed over the past forty years. These methods can be divided into three groups: analytical methods [7], graphical methods [8] and numerical methods [9]. The graphical and analytical methods are only applicable under various simplifying assumptions, and thus their value is limited in practical scenarios. In particular, the graphical and analytical methods cannot deal with the cavitation caused by negative pressure [10]. Numerical methods for simulating water hammer include the fluid-structure interaction method [11], the method of characteristics [12, 13], the heterogenous multiscale method [14], the finite volume method [15], and the wave plan method [16]. In this paper, we apply the method of lines [17, 18] to approximate the water hammer PDEs by a system of ODEs. This approach enables the application of ODE optimal control techniques, for which there are many existing high-quality numerical algorithms, to determine optimal valve closure strategies to mitigate water hammer.

To protect a pipeline system from water hammer effects, various passive protection strategies can be employed. These include using special materials to reinforce the pipeline and installing special devices such as relief valves, air chambers, and surge tanks [19]. However, the success of these strategies depends heavily on the characteristics of the pipeline system and on the experience of the designer/operator [20]. Moreover, although passive protection strategies can act as a guard against water hammer, it is usually better to try and prevent water hammer from occurring in the first place. Hence, effective control strategies for valve closure are required to avoid the worst effects of water hammer, such as hazardous pipeline collapse.

The water hammer process involves nonlinearities and is non-uniform in space and time. Therefore, optimal flow control requires a forecasting model capable of predicting the non-uniform and unsteady water flow in space and time. Furthermore, due to flow nonlinearities, it is difficult to establish the relationship between the control action and the corresponding response in the hydrodynamic variables. Thus, effective valve control strategies are essential. Cao [21] used functional extremum theory and the Ritz method to design optimal rules for both velocity change and valve closure to minimize the peak pressure at the valve. Axworthy [22] developed a valve closure algorithm for node-based, graph-theoretic models that can be applied within a slow transient (rigid water column) pipeline network. Tian [23] investigated the optimum design of parallel pump feedwater systems in nuclear power plants to mitigate the potential damage caused by valve-induced water hammer. Feng [24] proposed an optimal control method for the regulation of multiple valves, focusing on the active causes of water hammer. Now, with the rapid development of modern control theory and numerical methodologies, advances in nonlinear optimization have made the solution of nonlinear flow control problems possible. Accordingly, in this paper, we propose an effective numerical approach to determine optimal boundary controls for valve closure in fluid pipelines.

The paper is organized as follows. In Section 2, we introduce a hyperbolic PDE system to describe the fluid flow dynamics in the pipeline, after which we propose an optimal control problem for water hammer suppression during valve closure. In Section 3, we use the method of lines to approximate the hyperbolic PDE system by a non-stationary state space ODE model. Then, in Section 4, we use the control parameterization method, with both piecewise-linear and piecewise-quadratic basis functions, to solve the optimal control problem by designing the boundary controller to minimize pressure fluctuation. Finally, in Section 5, we give numerical results to demonstrate the superiority of the optimal boundary control strategy compared with the non-optimal (but widely-used) strategy of abruptly shutting off the valve.

2. Problem Formulation

2.1. Mathematical Model

We consider the situation shown in Figure 2, where a pipeline of length L is used to transport fluid from a reservoir to a terminus connected to a larger pipeline network. Let $l \in [0, L]$ denote the spatial variable along the pipeline, and let $t \in [0, T]$ denote the time variable. By neglecting the effects of viscosity, turbulence, and temperature variation, the flow along the pipeline can be described by the following hyperbolic PDE system [25, 26, 27], which consists of a momentum equation and a continuity equation:

$$\frac{\partial v(l,t)}{\partial t} = -\frac{1}{\rho}\frac{\partial p(l,t)}{\partial l} - \frac{f v(l,t)\,|v(l,t)|}{2D}, \tag{1a}$$

$$\frac{\partial p(l,t)}{\partial t} = -\rho c^2 \frac{\partial v(l,t)}{\partial l}, \tag{1b}$$

where v is the flow velocity, p is the edge pressure drop, D is the diameter of the pipeline, c is the wave velocity, f is the Darcy-Weisbach friction factor and ρ is the flow density. The boundary conditions for system (1) are

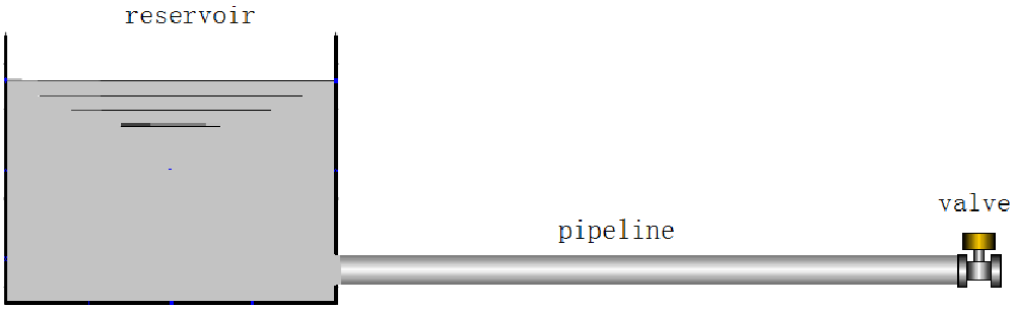

Figure 2: General layout of the pipeline system described in Section 2.1

$$p(0,t) = P, \quad v(L,t) = u(t), \quad t \in [0,T], \tag{2}$$

where P is the pressure generated by the reservoir (a given constant), and $u(t)$ is a boundary control variable that models actuation from a valve situated at the pipeline terminus. Our interest is in modeling the fluid flow during the valve closure period, which begins at $t = 0$ and ends at $t = T$. The boundary control, which must be manipulated to implement the valve closure, is required to satisfy the following bound constraint:

$$0 \leq u(t) \leq u_{\max}, \quad t \in [0,T], \tag{3}$$

where $u_{\max}$ denotes the maximum velocity. The rate of change in the boundary control is also subject to lower and upper bounds:

$$-\dot{u}_{\max} \leq \dot{u}(t) \leq \dot{u}_{\max}, \quad t \in [0,T], \tag{4}$$

where $\dot{u}_{\max}$ is a given constant. Since we require the valve to be completely closed at the terminal time,

$$u(T) = 0. \tag{5}$$

Any continuous function $u : [0,T] \to \mathbb{R}$ that is differentiable almost everywhere and satisfies (3)-(5) is called an admissible boundary control policy.

The initial conditions for system (1) are

$$p(l,0) = \overline{p}_0(l), \quad v(l,0) = \overline{v}_0(l), \quad l \in [0,L], \tag{6}$$

where $\overline{p}_0(l)$ and $\overline{v}_0(l)$ are given functions describing the initial state of the pipeline.

2.2. The Optimal Boundary Control Problem

Since closing the valve suddenly could cause severe water hammer effects, the boundary control $u(t)$ must be manipulated carefully to minimize pressure fluctuation. To this end, we consider the following objective function as proposed in references [28, 29]:

$$\begin{aligned} J = (p(L,T) - \hat{p}(L))^{2\gamma} + \frac{1}{T}\int_0^T (p(L,t) - \hat{p}(L))^{2\gamma} dt \\ + \frac{1}{LT}\int_0^T \int_0^L (p(l,t) - \hat{p}(l))^{2\gamma} dx dt, \end{aligned} \tag{7}$$

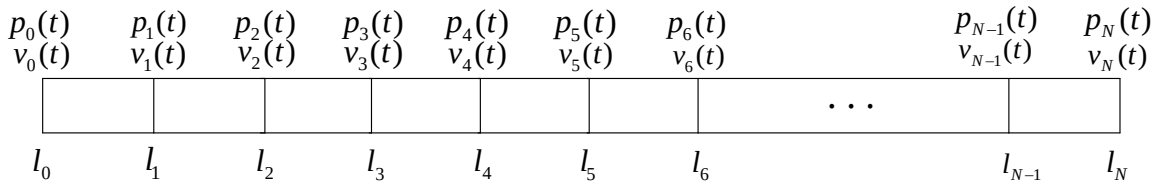

Figure 3: Pipeline spatial discretization using the method of lines

where γ is a positive integer and $\hat{p}(l)$ is a given function expressing the target pressure profile along the pipeline. The objective function (7) penalizes deviation between the actual pressure in the pipeline and the target pressure profile: the first term in (7) penalizes pressure deviation at the valve at the terminal time, the second term penalizes pressure deviation at the valve across the entire time horizon, and the third term penalizes global pressure deviation over the entire pipeline length and time horizon. The reason for placing special emphasis in (7) at the valve location is that the valve will normally contain sensitive electrical components that must be protected. Our optimal boundary control problem is now defined as follows.

Problem $\mathbf{P}_0$. *Given the system (1) with boundary conditions (2) and initial conditions (6), choose the boundary control $u : [0, T] \to \mathbb{R}$ to minimize the objective function (7) subject to the bound constraints (3) and (4) and the terminal control constraint (5).*

3. Spatial Discretization

To simplify Problem P_0, we will use the method of lines to approximate the PDE model by a state space ODE model. First, we decompose the pipeline into equally-spaced intervals $[l_{i-1}, l_i], i = 1, \ldots, N$, where N is an even integer and $l_0 = 0$ and $l_N = L$. Define

$$v_i(t) = v(l_i, t), \quad i = 0, \ldots, N,$$

and

$$p_i(t) = p(l_i, t), \quad i = 0, \ldots, N.$$

These definitions, along with the spatial node points, are shown in Figure 3.

Based on the definitions of v_i and p_i, we obtain the following finite difference approximations:

$$\frac{\partial p(l_i, t)}{\partial l} = \frac{p_{i+1}(t) - p_i(t)}{\Delta l}, \quad i = 0, \ldots, N-1, \tag{8a}$$

$$\frac{\partial v(l_i, t)}{\partial l} = \frac{v_i(t) - v_{i-1}(t)}{\Delta l}, \quad i = 1, \ldots, N, \tag{8b}$$

where $\Delta l = L/N$. Substituting the finite difference approximations (8a) and (8b) into the PDE model (1a) and (1b) yields

$$\dot{v}_i(t) = \frac{1}{\rho \Delta l}(p_i(t) - p_{i+1}(t)) - \frac{f v_i(t) \, |v_i(t)|}{2D}, \quad i = 0, \ldots, N-1, \tag{9a}$$

$$\dot{p}_i(t) = \frac{\rho c^2}{\Delta l}(v_{i-1}(t) - v_i(t)), \quad i = 1, \ldots, N. \tag{9b}$$

By virtue of the definitions of v_i and p_i, the boundary conditions (2) become

$$p_0(t) = P,\ v_N(t) = u(t), \quad t \in [0, T]. \tag{10}$$

To simplify the notation, let

$$\mathbf{x}(t) = \left[\ p_1(t) \quad \cdots \quad p_N(t) \quad v_0(t) \quad \cdots \quad v_{N-1}(t)\ \right]^T \in \mathbb{R}^{2N},$$

$$|\mathbf{x}(t)| = \left[\ |p_1(t)| \quad \cdots \quad |p_N(t)| \quad |v_0(t)| \quad \cdots \quad |v_{N-1}(t)|\ \right]^T \in \mathbb{R}^{2N}.$$

Then, by using the boundary conditions (10), equations (9a) and (9b) can be written in compact form as

$$\dot{\mathbf{x}}(t) = A\mathbf{x}(t) + u(t)\mathbf{a} + P\mathbf{b} + B\mathbf{x}(t) \circ |\mathbf{x}(t)|\,, \tag{11}$$

where $\circ$ denotes the Hadamard product, and

$$A = \begin{bmatrix} 0 & A_{12} \\ A_{21} & 0 \end{bmatrix} \in \mathbb{R}^{2N\times 2N},$$

$$A_{12} = \frac{\rho c^2}{\Delta l}\begin{bmatrix} 1 & -1 & 0 & \cdots & 0 & 0 \\ 0 & 1 & -1 & \cdots & 0 & 0 \\ 0 & 0 & 1 & \cdots & 0 & 0 \\ \vdots & \vdots & \vdots & \ddots & \vdots & \vdots \\ 0 & 0 & 0 & \cdots & 1 & -1 \\ 0 & 0 & 0 & \cdots & 0 & 1 \end{bmatrix} \in \mathbb{R}^{N\times N},$$

$$A_{21} = \frac{1}{\rho\Delta l}\begin{bmatrix} -1 & 0 & 0 & \cdots & 0 & 0 \\ 1 & -1 & 0 & \cdots & 0 & 0 \\ 0 & 1 & -1 & \cdots & 0 & 0 \\ \vdots & \vdots & \vdots & \ddots & \vdots & \vdots \\ 0 & 0 & 0 & \cdots & -1 & 0 \\ 0 & 0 & 0 & \cdots & 1 & -1 \end{bmatrix} \in \mathbb{R}^{N\times N},$$

$$\mathbf{a} = \left[\ 0 \quad \cdots \quad -\tfrac{\rho c^2}{\Delta l} \quad 0 \quad \cdots \quad 0\ \right]^T \in \mathbb{R}^{2N},$$

$$\mathbf{b} = \left[\ 0 \quad \cdots \quad 0 \quad \tfrac{1}{\rho\Delta l} \quad \cdots \quad 0\ \right]^T \in \mathbb{R}^{2N},$$

$$B = -\frac{f}{2D}\begin{bmatrix} 0 & 0 \\ 0 & I \end{bmatrix} \in \mathbb{R}^{2N},$$

and I is the $N \times N$ identity matrix. The initial conditions (6) become

$$\mathbf{x}(0) = \left[\ \overline{p}_0(l_1) \quad \cdots \quad \overline{p}_0(l_N) \quad \overline{v}_0(l_0) \quad \cdots \quad \overline{v}_0(l_{N-1})\ \right]^T \in \mathbb{R}^{2N}. \tag{12}$$

Furthermore, using Simpson's rule [30], the objective function (7) becomes

$$\begin{aligned} J = (x_N(T) - \hat{p}(L))^{2\gamma} + \int_0^T \Bigg\{ & \frac{3N+1}{3NT}(x_N(t) - \hat{p}(L))^{2\gamma} \\ & + \frac{1}{3TN}(P - \hat{p}(0))^{2\gamma} + \frac{4}{3TN}\sum_{j=1}^{N/2}(x_{2j-1}(t) - \hat{p}(l_{2j-1}))^{2\gamma} \\ & + \frac{2}{3TN}\sum_{j=1}^{N/2-1}(x_{2j}(t) - \hat{p}(l_{2j}))^{2\gamma}\Bigg\} dt. \end{aligned} \tag{13}$$

Note that the term $(P-\hat{p}(0))^{2\gamma}$ in the integral is a constant. Hence, instead of minimizing (13), we can equivalently minimize the following modified objective function:

$$J = (x_N(T) - \hat{p}(L))^{2\gamma} + \int_0^T \left\{ \frac{3N+1}{3NT}(x_N(t) - \hat{p}(L))^{2\gamma} + \frac{4}{3TN}\sum_{j=1}^{N/2}(x_{2j-1}(t) - \hat{p}(l_{2j-1}))^{2\gamma} + \frac{2}{3TN}\sum_{j=1}^{N/2-1}(x_{2j}(t) - \hat{p}(l_{2j}))^{2\gamma} \right\} dt. \tag{14}$$

Our approximate problem is now stated as follows.

Problem $\mathbf{P}_N$. *Given the system (11) with initial condition (12), choose the optimal control $u : [0,T] \to \mathbb{R}$ to minimize the objective function (14) subject to the bound constraints (3) and (4) and the terminal control constraint (5).*

4. Control Parameterization

Problem P_N is a conventional optimal control problem governed by ODEs. To solve Problem P_N numerically, we will use the control parameterization method [31], which involves approximating the control by a linear combination of basis functions, where the coefficients in the linear combination are decision variables to be optimized. Then, by exploiting special formulae for the gradient of the objective function, the resulting approximate problem can be solved using standard gradient-based optimization techniques [32].

Control parameterization is normally applied with piecewise-constant basis functions [32]. However, piecewise-constant control approximation is not suitable for Problem P_N because the boundary controller in Problem P_N is required to be continuous. Thus, we instead develop two continuous approximation schemes: one with piecewise-linear basis functions, the other with piecewise-quadratic basis functions.

4.1. Piecewise-Linear Control Parameterization

For piecewise-linear control parameterization [33], we approximate the derivative of the boundary control as follows:

$$\dot{u}(t) \approx \sigma^k, \quad t \in [t_{k-1}, t_k), \quad k = 1, \ldots, r, \tag{15}$$

where $r > 1$ is the number of approximation subintervals, $[t_{k-1}, t_k)$ is the kth approximation subinterval, and σ^k is the rate of change of the control on the kth subinterval. Moreover, $t_k,\ k = 0, \ldots, r$, are fixed knot points such that

$$0 = t_0 < t_1 < t_2 < \cdots < t_{r-1} < t_r = T. \tag{16}$$

We can write equation (15) as

$$\dot{u}(t) \approx \sum_{k=1}^{r} \sigma^k \chi_{[t_{k-1}, t_k)}(t), \tag{17}$$

where $\chi_{[t_{k-1},t_k)}(t)$ is the indicator function defined by

$$\chi_{[t_{k-1},t_k)}(t) = \begin{cases} 1, & \text{if } t \in [t_{k-1}, t_k), \\ 0, & \text{otherwise.} \end{cases} \tag{18}$$

With $\dot{u}(t)$ approximated by a piecewise-constant function according to (17), $u(t)$ is piecewise-linear with jumps in the derivative at $t = t_1, t_2, \ldots, t_{r-1}$. Let $x_{2N+1}(t) = u(t)$ be a new state variable. Then $x_{2N+1}(t)$ is governed by the following dynamics:

$$\dot{x}_{2N+1}(t) = \sum_{k=1}^{r} \sigma^k \chi_{[t_{k-1},t_k)}(t), \quad t \in [0, T], \tag{19a}$$

$$x_{2N+1}(0) = u_0, \tag{19b}$$

where $u_0 = u_{\max}$ is the initial value of $u(t)$. In view of (3), we require the following continuous state inequality constraint:

$$0 \leq x_{2N+1}(t) \leq u_{\max}, \quad t \in [0, T]. \tag{20}$$

Clearly, since $x_{2N+1}(t)$ is piecewise-linear with break points at $t = t_1, t_2, \ldots, t_{r-1}$, this continuous state inequality constraint is equivalent to the following constraints:

$$0 \leq x_{2N+1}(t_k) \leq u_{\max}, \quad k = 1, \ldots, r. \tag{21}$$

Such constraints are known as canonical constraints in the optimal control literature [32].

Under the piecewise-linear control parameterization scheme (17), the constraints (4) become

$$-\dot{u}_{\max} \leq \sigma^k \leq \dot{u}_{\max}, \quad k = 1, \ldots, r. \tag{22}$$

In addition, the dynamic system (11) becomes

$$\dot{\mathbf{x}}(t) = A\mathbf{x}(t) + x_{2N+1}(t)\mathbf{a} + P\mathbf{b} + B\mathbf{x}(t) \circ |\mathbf{x}(t)|, \quad t \in [0, T]. \tag{23}$$

Furthermore, the terminal control constraint (5) becomes the following terminal state constraint:

$$x_{2N+1}(T) = 0. \tag{24}$$

Our approximate problem is defined as follows.

Problem $\mathbf{P}_N^r$. *Given the system defined by (19), (23), and (12), choose the control parameter vector* $\boldsymbol{\sigma} = \begin{bmatrix} \sigma^1 & \cdots & \sigma^r \end{bmatrix} \in \mathbb{R}^r$ *to minimize the objective function (14) subject to the bound constraints (22) and the state constraints (21) and (24).*

4.2. Solving Problem P_N^r

The approximate problem defined in Section 4.1 is a nonlinear optimization problem in which a finite number of decision variables need to be chosen to minimize an objective function subject to a set of constraints. For this approximate problem, the objective function is an implicit—rather than explicit—function of the decision variables. Thus, computing the gradient of the objective function, as required to solve the approximate

problem using gradient-based optimization methods such as SQP, is a non-trivial task. Nevertheless, we will now show that this gradient can be computed using the sensitivity approach described in [34, 35]. Then, the SQP method can be applied to generate search directions that lead to profitable areas of the search space [36].

First, let $\mathbf{x}^r(\cdot|\boldsymbol{\sigma})$ and $x^r_{2N+1}(\cdot|\boldsymbol{\sigma})$ denote the solution of the enlarged system defined by (19), (23), and (12) corresponding to the control parameter vector $\boldsymbol{\sigma} = \begin{bmatrix} \sigma^1 & \cdots & \sigma^r \end{bmatrix}$. Then we have the following result.

Theorem 1. *For each $m = 1, \ldots, r$, the state variation of $x^r_{2N+1}(\cdot|\boldsymbol{\sigma})$ on the interval $[t_{m-1}, t_m]$ is given by*

$$\frac{\partial x^r_{2N+1}(t|\boldsymbol{\sigma})}{\partial \sigma^k} = \begin{cases} t - t_{m-1}, & \text{if } k = m, \\ t_k - t_{k-1}, & \text{if } k < m, \\ 0, & \text{if } k > m. \end{cases} \tag{25}$$

Proof. The proof is by induction. For $m = 1$, it follows from (19) that

$$x^r_{2N+1}(t|\boldsymbol{\sigma}) = u_{\max} + \sigma^1(t - t_0) = u_{\max} + \sigma^1 t, \quad t \in [0, t_1]. \tag{26}$$

Then clearly, for all $t \in [0, t_1]$,

$$\frac{\partial x^r_{2N+1}(t|\boldsymbol{\sigma})}{\partial \sigma^k} = \begin{cases} t, & \text{if } k = 1, \\ 0, & \text{if } k > 1, \end{cases} \tag{27}$$

which shows that (25) is satisfied for $m = 1$. Now, suppose that (25) holds for $m = q$. Then for all $t \in [t_{q-1}, t_q]$,

$$\frac{\partial x^r_{2N+1}(t|\boldsymbol{\sigma})}{\partial \sigma^k} = \begin{cases} t - t_{q-1}, & \text{if } k = q, \\ t_k - t_{k-1}, & \text{if } k < q, \\ 0, & \text{if } k > q. \end{cases} \tag{28}$$

For $m = q + 1$, equation (19a) implies

$$x^r_{2N+1}(t|\boldsymbol{\sigma}) = x^r_{2N+1}(t_q|\boldsymbol{\sigma}) + \sigma^{q+1}(t - t_q), \quad t \in [t_q, t_{q+1}]. \tag{29}$$

Hence, for all $t \in [t_q, t_{q+1}]$,

$$\frac{\partial x^r_{2N+1}(t|\boldsymbol{\sigma})}{\partial \sigma^k} = \begin{cases} t - t_q, & \text{if } k = q + 1, \\ \frac{\partial x^r_{2N+1}(t_q|\boldsymbol{\sigma})}{\partial \sigma^k}, & \text{if } k < q + 1, \\ 0, & \text{if } k > q + 1. \end{cases} \tag{30}$$

Applying the inductive hypothesis yields

$$\frac{\partial x^r_{2N+1}(t|\boldsymbol{\sigma})}{\partial \sigma^k} = \begin{cases} t - t_q, & \text{if } k = q + 1, \\ t_k - t_{k-1}, & \text{if } k < q + 1, \\ 0, & \text{if } k > q + 1. \end{cases} \tag{31}$$

This shows that (25) holds for $m = q + 1$. Thus, the result follows from mathematical induction. □

Clearly,

$$\frac{\partial \mathbf{x}^r(t|\boldsymbol{\sigma})}{\partial \sigma^k} = \mathbf{0}, \quad t \in [0, t_{k-1}]. \tag{32}$$

Moreover, for each $m = k, k+1, \ldots, r$,

$$\begin{aligned} \mathbf{x}^r(t|\boldsymbol{\sigma}) = \mathbf{x}^r(t_{m-1}|\boldsymbol{\sigma}) + \int_{t_{m-1}}^{t} \Big\{ & A\mathbf{x}^r(s|\boldsymbol{\sigma}) + \mathbf{a}x^r_{2N+1}(s|\boldsymbol{\sigma}) \\ & + \mathbf{b}P + B\mathbf{x}^r(s|\boldsymbol{\sigma}) \circ |\mathbf{x}^r(s|\boldsymbol{\sigma})| \Big\} ds, \quad t \in [t_{m-1}, t_m]. \end{aligned} \tag{33}$$

Differentiating (33) with respect to σ^k gives

$$\begin{aligned} \frac{\partial \mathbf{x}^r(t|\boldsymbol{\sigma})}{\partial \sigma^k} = \frac{\partial \mathbf{x}^r(t_{m-1}|\boldsymbol{\sigma})}{\partial \sigma^k} + \int_{t_{m-1}}^{t} \Bigg\{ & A\frac{\partial \mathbf{x}^r(s|\boldsymbol{\sigma})}{\partial \sigma^k} + \mathbf{a}\frac{\partial x^r_{2N+1}(s|\boldsymbol{\sigma})}{\partial \sigma^k} \\ & + 2B\,|\mathbf{x}^r(s|\boldsymbol{\sigma})| \circ \frac{\partial \mathbf{x}^r(s|\boldsymbol{\sigma})}{\partial \sigma^k} \Bigg\} ds, \quad t \in [t_{m-1}, t_m), \quad m = k, k+1, \ldots, r. \end{aligned} \tag{34}$$

Thus, differentiating (34) with respect to time t, we obtain

$$\begin{aligned} \frac{d}{dt}\left\{\frac{\partial \mathbf{x}^r(t|\boldsymbol{\sigma})}{\partial \sigma^k}\right\} = & A\frac{\partial \mathbf{x}^r(t|\boldsymbol{\sigma})}{\partial \sigma^k} + \mathbf{a}\frac{\partial x^r_{2N+1}(t|\boldsymbol{\sigma})}{\partial \sigma^k} \\ & + 2B\,|\mathbf{x}^r(t|\boldsymbol{\sigma})| \circ \frac{\partial \mathbf{x}^r(t|\boldsymbol{\sigma})}{\partial \sigma^k}, \quad t \in [t_{m-1}, t_m), \quad m = k, k+1, \ldots, r. \end{aligned} \tag{35}$$

Based on (32) and (35), we have the following result.

Theorem 2. *The state variation of $\mathbf{x}^r(\cdot|\boldsymbol{\sigma})$ with respect to σ^k is the solution $\Gamma^k(\cdot|\boldsymbol{\sigma})$ of the following sensitivity system:*

$$\begin{aligned} \dot{\Gamma}^k(t) = A\Gamma^k(t) + \mathbf{a}\frac{\partial x^r_{2N+1}(t|\boldsymbol{\sigma})}{\partial \sigma^k} + 2B\,|\mathbf{x}^r(t|\boldsymbol{\sigma})| \circ \Gamma^k(t), \\ t \in [t_{m-1}, t_m), \quad m = k, k+1, \ldots, r, \end{aligned} \tag{36}$$

where $\Gamma^k(t) = 0$, $t \in [0, t_{k-1})$ and $\frac{\partial x^r_{2N+1}(t|\boldsymbol{\sigma})}{\partial \sigma^k}$ is given by the formula in Theorem 1.

Clearly, the gradients of constraints (21) and (24) can be computed using Theorem 1. For the objective function, the gradient can be obtained by differentiating (14) using the chain rule:

$$\begin{aligned} \frac{\partial J(\boldsymbol{\sigma})}{\partial \sigma^k} = & 2\gamma(x_N(T) - \hat{p}(L))^{2\gamma-1}\Gamma^k_N(T\,|\boldsymbol{\sigma}) \\ & + \int_0^T \Bigg\{ \frac{2\gamma(3N+1)}{3NT}(x_N(t) - \hat{p}(L))^{2\gamma-1}\Gamma^k_N(t\,|\boldsymbol{\sigma}) \\ & + \frac{8\gamma}{3NT}\sum_{j=1}^{N/2}(x_{2j-1}(t) - \hat{p}(l_{2j-1}))^{2\gamma-1}\Gamma^k_{2j-1}(t\,|\boldsymbol{\sigma}) \\ & + \frac{4\gamma}{3NT}\sum_{j=1}^{N/2-1}(x_{2j}(t) - \hat{p}(l_{2j}))^{2\gamma-1}\Gamma^k_{2j}(t\,|\boldsymbol{\sigma}) \Bigg\} dt. \end{aligned}$$

By incorporating these gradient formulae with a nonlinear programming algorithm such as SQP, Problem P^r_N can be solved efficiently. The gradient-based optimization framework is illustrated in Figure 4. Convergence results showing that the solution of Problem P^r_N converges to the solution of Problem P_N are derived in [37, 38, 39].

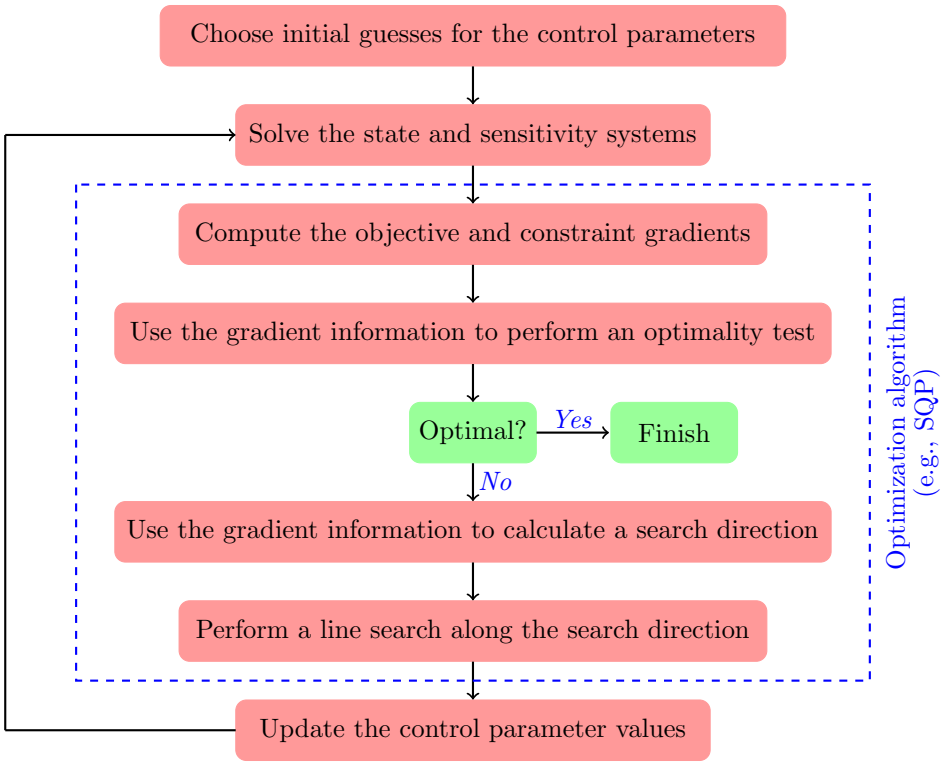

Figure 4: Gradient-based optimization framework for solving Problem P_N^r

4.3. Piecewise-Quadratic Control Parameterization

For piecewise-quadratic control parameterization, we approximate the second derivative of the control instead of the first derivative:

$$\ddot{u}(t) \approx \sum_{k=1}^{r} \hat{\sigma}^k \chi_{[t_{k-1},t_k)}(t), \quad t \in [0,T]. \tag{37}$$

Then, we introduce two new state variables $x_{2N+1}(t)$ and $x_{2N+2}(t)$ governed by the following dynamics:

$$\dot{x}_{2N+1}(t) = x_{2N+2}(t), \quad t \in [0,T], \tag{38a}$$
$$x_{2N+1}(0) = u_0, \tag{38b}$$
$$\dot{x}_{2N+2}(t) = \sum_{k=1}^{r} \hat{\sigma}^k \chi_{[t_{k-1},t_k)}(t), \quad t \in [0,T], \tag{38c}$$
$$x_{2N+2}(0) = \dot{u}_0, \tag{38d}$$

where u_0 and $\dot{u}_0$ are given constants. Here, $x_{2N+2}(t)$ represents $\dot{u}(t)$ (a piecewise-linear function) and $x_{2N+1}(t)$ represents $u(t)$ (a piecewise-quadratic function). Thus, $u_0 = u_{\max}$ (the valve is initially fully open) and $\dot{u}_0$ is the initial value of $\dot{u}(t)$. In view of (3) and (4), we have the following continuous state inequality constraints:

$$0 \le x_{2N+1}(t) \le u_{\max}, \quad t \in [0,T], \tag{39}$$

and

$$-\dot{u}_{\max} \leq x_{2N+2}(t) \leq \dot{u}_{\max}, \quad t \in [0, T]. \tag{40}$$

Since $x_{2N+2}(t)$ is piecewise-linear, the continuous state inequality constraint (40) is equivalent to:

$$-\dot{u}_{\max} \leq x_{2N+2}(t_k) \leq \dot{u}_{\max}, \quad k = 1, \ldots, r. \tag{41}$$

After applying the piecewise-quadratic control parameterization scheme, the dynamic system (11) becomes

$$\dot{\mathbf{x}}(t) = A\mathbf{x}(t) + x_{2N+1}(t)\mathbf{a} + P\mathbf{b} + B\mathbf{x}(t) \circ |\mathbf{x}(t)|, \quad t \in [0, T]. \tag{42}$$

Furthermore, the terminal control constraint (5) becomes the following terminal state constraint:

$$x_{2N+1}(T) = 0. \tag{43}$$

Our approximate problem is defined as follows.

Problem Q^r_N. *Given the system defined by (38), (42), and (12), choose the control parameter vector $\hat{\boldsymbol{\sigma}} = \begin{bmatrix} \hat{\sigma}^1 & \cdots & \hat{\sigma}^r \end{bmatrix} \in \mathbb{R}^r$ to minimize the objective function (14) subject to the state constraints (39), (41) and (43).*

4.4. Solving Problem Q^r_N

Like Problem P^r_N, Problem Q^r_N is a nonlinear optimization problem. The only significant difference is that Problem Q^r_N contains a continuous inequality state constraint (39) that cannot be converted into a finite number of conventional constraints. To address this difficulty, we first note that (39) is equivalent to the following non-smooth integral constraints:

$$\int_0^T \max\{-x_{2N+1}(t), 0\}dt = 0, \quad \int_0^T \max\{x_{2N+1}(t) - u_{\max}, 0\}dt = 0. \tag{44}$$

Since the $\max\{\cdot, 0\}$ function is non-smooth, we use the following smooth approximation scheme defined in [39]:

$$\max\{y, 0\} \approx \phi_\alpha(y) = \frac{1}{2}\sqrt{y^2 + 4\alpha^2} + \frac{1}{2}y, \tag{45}$$

where $\alpha > 0$ is a smoothing parameter. Note that $\phi_\alpha(y) \geq 0$ for all y. Based on this approximation scheme, we append constraints (44) to the objective (14) to obtain the following penalty function:

$$G_{\alpha,\omega}(\hat{\boldsymbol{\sigma}}) = J(\hat{\boldsymbol{\sigma}}) + \omega\left\{\int_0^T \phi_\alpha(-x_{2N+1}(t))dt + \int_0^T \phi_\alpha(x_{2N+1}(t) - u_{\max})dt\right\}, \tag{46}$$

where $\omega > 0$ is a penalty parameter. We now define an approximation of Problem Q^r_N as follows.

Problem $\mathrm{Q}^r_{N,\alpha,\omega}$. *Given the system defined by (38), (42), and (12), choose the control parameter vector $\hat{\boldsymbol{\sigma}} = \begin{bmatrix} \hat{\sigma}^1 & \cdots & \hat{\sigma}^r \end{bmatrix} \in \mathbb{R}^r$ to minimize the penalty function (46) subject to the state constraints (41) and (43).*

Note that when α is small, $\phi_\alpha(y)$ is a good approximation of $\max\{y, 0\}$, and thus Problem $\mathrm{Q}^r_{N,\alpha,\omega}$ is a good approximation of Problem Q^r_N. Formal convergence results are given in [39].

Let $\mathbf{x}^r(\cdot|\hat{\boldsymbol{\sigma}})$, $x^r_{2N+1}(\cdot|\hat{\boldsymbol{\sigma}})$, and $x^r_{2N+2}(\cdot|\hat{\boldsymbol{\sigma}})$ denote the solution of the enlarged system defined by (38), (42), and (12) corresponding to the control parameter vector $\hat{\boldsymbol{\sigma}} = \begin{bmatrix} \hat{\sigma}^1 & \cdots & \hat{\sigma}^r \end{bmatrix}$. Based on Theorem 1, for $t \in [t_{m-1}, t_m]$,

$$\frac{\partial x^r_{2N+2}(t|\hat{\boldsymbol{\sigma}})}{\partial \hat{\sigma}^k} = \begin{cases} t - t_{m-1}, & \text{if } k = m, \\ t_k - t_{k-1}, & \text{if } k < m, \\ 0, & \text{if } k > m. \end{cases} \tag{47}$$

The derivative of $x^r_{2N+1}(t|\hat{\boldsymbol{\sigma}})$ is given in the following theorem.

Theorem 3. *For each $m = 1, \ldots, r$, the state variation of $x^r_{2N+1}(\cdot|\hat{\boldsymbol{\sigma}})$ on the interval $[t_{m-1}, t_m]$ is given by*

$$\frac{\partial x^r_{2N+1}(t|\hat{\boldsymbol{\sigma}})}{\partial \hat{\sigma}^k} = \begin{cases} \frac{1}{2}t^2 - t_{m-1}t + \frac{1}{2}t^2_{m-1}, & \textit{if } k = m, \\ (t_k - t_{k-1})t + \frac{1}{2}t^2_{k-1} - \frac{1}{2}t^2_k, & \textit{if } k < m, \\ 0, & \textit{if } k > m. \end{cases} \tag{48}$$

Proof. The proof is by induction on m. For $m = 1$,

$$x^r_{2N+1}(t|\hat{\boldsymbol{\sigma}}) = u_0 + \int_0^t x^r_{2N+2}(s|\hat{\boldsymbol{\sigma}})ds, \quad t \in [0, t_1]. \tag{49}$$

Thus, using (47), for all $t \in [0, t_1]$,

$$\frac{\partial x^r_{2N+1}(t|\hat{\boldsymbol{\sigma}})}{\partial \hat{\sigma}^k} = \int_0^t \frac{\partial x^r_{2N+2}(s|\hat{\boldsymbol{\sigma}})}{\partial \hat{\sigma}^k} ds = \begin{cases} \frac{1}{2}t^2, & \text{if } k = 1, \\ 0, & \text{if } k > 1. \end{cases} \tag{50}$$

This shows that (48) is satisfied for $m = 1$. Now, suppose that (48) holds for $m = q$. Then for all $t \in [t_{q-1}, t_q]$,

$$\frac{\partial x^r_{2N+1}(t|\hat{\boldsymbol{\sigma}})}{\partial \hat{\sigma}^k} = \begin{cases} \frac{1}{2}t^2 - t_{q-1}t + \frac{1}{2}t^2_{q-1}, & \text{if } k = q, \\ (t_k - t_{k-1})t + \frac{1}{2}t^2_{k-1} - \frac{1}{2}t^2_k, & \text{if } k < q, \\ 0, & \text{if } k > q. \end{cases} \tag{51}$$

For $t \in [t_q, t_{q+1}]$,

$$x^r_{2N+1}(t|\hat{\boldsymbol{\sigma}}) = x^r_{2N+1}(t_q|\hat{\boldsymbol{\sigma}}) + \int_{t_q}^t x^r_{2N+2}(s|\hat{\boldsymbol{\sigma}})ds. \tag{52}$$

Differentiating (52) with respect to $\hat{\sigma}^k$ gives

$$\frac{\partial x^r_{2N+1}(t|\hat{\boldsymbol{\sigma}})}{\partial \hat{\sigma}^k} = \frac{\partial x^r_{2N+1}(t_q|\hat{\boldsymbol{\sigma}})}{\partial \hat{\sigma}^k} + \int_{t_q}^t \frac{\partial x^r_{2N+2}(s|\hat{\boldsymbol{\sigma}})}{\partial \hat{\sigma}^k} ds. \tag{53}$$

Thus, if $k > q+1$, then clearly

$$\frac{\partial x^r_{2N+1}(t|\hat{\boldsymbol{\sigma}})}{\partial \hat{\sigma}^k} = 0. \tag{54}$$

If $k = q+1$, then by using (47) and (51) to simplify (53), we obtain

$$\frac{\partial x^r_{2N+1}(t|\hat{\boldsymbol{\sigma}})}{\partial \hat{\sigma}^k} = \int_{t_q}^{t} (s - t_q)ds = \frac{1}{2}t^2 - t_q t + \frac{1}{2}t_q^2. \tag{55}$$

Finally, if $k < q+1$, then the inductive hypothesis (51) implies

$$\begin{aligned}\frac{\partial x^r_{2N+1}(t_q|\hat{\boldsymbol{\sigma}})}{\partial \hat{\sigma}^k} &= \begin{cases} \frac{1}{2}t_q^2 - t_q t_{q-1} + \frac{1}{2}t_{q-1}^2, & \text{if } k = q, \\ (t_k - t_{k-1})t_q + \frac{1}{2}t_{k-1}^2 - \frac{1}{2}t_k^2, & \text{if } k < q, \end{cases} \\ &= (t_k - t_{k-1})t_q + \frac{1}{2}t_{k-1}^2 - \frac{1}{2}t_k^2.\end{aligned}$$

Thus, (53) becomes

$$\begin{aligned}\frac{\partial x^r_{2N+1}(t|\hat{\boldsymbol{\sigma}})}{\partial \hat{\sigma}^k} &= (t_k - t_{k-1})t_q + \frac{1}{2}t_{k-1}^2 - \frac{1}{2}t_k^2 + \int_{t_q}^{t} (t_k - t_{k-1})ds \\ &= (t_k - t_{k-1})t + \frac{1}{2}t_{k-1}^2 - \frac{1}{2}t_k^2.\end{aligned} \tag{56}$$

Equations (54), (55) and (56) show that (48) holds for $m = q+1$. Thus, the result follows from mathematical induction. □

The state variation of $\mathbf{x}^r(\cdot|\hat{\boldsymbol{\sigma}})$ in Problem $\mathrm{Q}^r_{N,\alpha,\omega}$ can be computed in the same manner as for Problem P^r_N. This leads to the following theorem (see Theorem 2).

Theorem 4. *The state variation of $\mathbf{x}^r(\cdot|\hat{\boldsymbol{\sigma}})$ with respect to $\hat{\sigma}^k$ is the solution $\Psi^k(\cdot|\hat{\boldsymbol{\sigma}})$ of the following sensitivity system:*

$$\begin{aligned}\dot{\Psi}^k(t) = A\Psi^k(t) + \mathbf{a}\frac{\partial x^r_{2N+1}(t|\hat{\boldsymbol{\sigma}})}{\partial \hat{\sigma}^k} + 2B\,|\mathbf{x}^r(t|\hat{\boldsymbol{\sigma}})\,| \circ \Psi^k(t), \\ t \in [t_{m-1}, t_m), \quad m = k, k+1, \ldots, r,\end{aligned} \tag{57}$$

where $\Psi^k(t) = 0$, $t \in [0, t_{k-1})$ and $\frac{\partial x^r_{2N+1}(t|\hat{\boldsymbol{\sigma}})}{\partial \hat{\sigma}^k}$ is given by the formula in Theorem 3.

Clearly, the gradients of constraints (41) and (43) can be computed using equations (47) and (48). For the penalty function (46), the gradient can be obtained using the chain rule of differentiation:

$$\begin{aligned}\frac{\partial G_{\alpha,\omega}(\hat{\boldsymbol{\sigma}})}{\partial \hat{\sigma}^k} &= 2\gamma(x_N(T) - \hat{p}(L))^{2\gamma-1}\Psi^k_N(T\,|\hat{\boldsymbol{\sigma}}\,) + \int_0^T \Bigg\{ \frac{2\gamma(3N+1)}{3NT}(x_N(t) - \hat{p}(L))^{2\gamma-1}\Psi^k_N(t\,|\hat{\boldsymbol{\sigma}}\,) \\ &\quad + \frac{8\gamma}{3NT}\sum_{j=1}^{N/2}(x_{2j-1}(t) - \hat{p}(l_{2j-1}))^{2\gamma-1}\Psi^k_{2j-1}(t\,|\hat{\boldsymbol{\sigma}}\,) \\ &\quad + \frac{4\gamma}{3NT}\sum_{j=1}^{N/2-1}(x_{2j}(t) - \hat{p}(l_{2j}))^{2\gamma-1}\Psi^k_{2j}(t\,|\hat{\boldsymbol{\sigma}}\,)\Bigg\}dt \\ &\quad + \omega\int_0^T \left\{ \frac{d\phi_\alpha(x_{2N+1}(t) - u_{\max})}{dy}\frac{\partial x_{2N+1}(t|\hat{\boldsymbol{\sigma}})}{\partial \hat{\sigma}^k} - \frac{d\phi_\alpha(-x_{2N+1}(t))}{dy}\frac{\partial x_{2N+1}(t|\hat{\boldsymbol{\sigma}})}{\partial \hat{\sigma}^k}\right\}dt,\end{aligned}$$

where $\frac{\partial x_{2N+1}(t|\hat{\boldsymbol{\sigma}})}{\partial \tilde{\sigma}^k}$ is given by the formula in Theorem 3. By incorporating these gradient formulae into a nonlinear programming algorithm such as SQP, Problem $\mathrm{Q}^r_{N,\alpha,\omega}$ can be solved efficiently. When α is small and ω is large, the solution of Problem $\mathrm{Q}^r_{N,\alpha,\omega}$ is a good approximation of the solution of Problem Q^r_N. See the convergence results in [39] for more details.

5. Numerical Simulations

For the numerical simulations, we consider a stainless steel pipeline of length $L = 20$ meters and diameter $D = 100$ millimeters. The flow density is taken as $\rho = 1000$ kg/m^3. Since the Darcy-Weisbach friction factor f for stainless steel pipelines is normally contained in the range $[0.02, 0.04]$ (see reference [40]), we choose $f = 0.03$. Moreover, as in [41], we choose $c = 1200$ m/s for the wave speed. The reservoir pressure is set at $P = 2 \times 10^5$ Pa, which corresponds to the pressure exerted by a fluid tower approximately 20 meters high. We assume that the pipeline fluid flow is initially in the steady state with constant velocity $\bar{v}_0(l) = 2$ m/s. It then follows from (1a) that

$$0 = -\frac{1}{\rho}\frac{\partial \bar{p}_0(l)}{\partial l} - \frac{2f}{D},$$

and thus

$$\frac{\partial \bar{p}_0(l)}{\partial l} = -\frac{2\rho f}{D}.$$

Integrating for $\bar{p}_0(l)$ yields

$$\bar{p}_0(l) = P - \frac{2\rho f}{D} l.$$

We choose $\gamma = 2$ in the objective function (14). In our numerical experience, larger values of γ have little effect on the results—this is consistent with the observations in reference [28], which advocates $\gamma = 2$ as the best choice. For the control bounds, we set $u_{\max} = 2$ and $\dot{u}_{\max} = 10$, and for the terminal time, we set $T = 10$ seconds. Moreover, we define $\hat{p}(l) = P = 2 \times 10^5$ Pa as the target pressure profile, since when the valve is completely closed the pressure will be constant across the pipeline (and equal to the reservoir pressure) in steady state.

Our numerical simulation study was carried out within the MATLAB programming environment (version R2010b) running on a personal computer with the following configuration: Intel Core i5-2320 3.00GHz CPU, 4.00GB RAM, 64-bit Windows 7 Operating System. Our MATLAB code implements the gradient-based optimization procedure in Figure 4 by combining FMINCON with the sensitivity method for gradient computation.

5.1. Piecewise-Linear Control Parameterization

Using the piecewise-linear control parameterization method with $r = 10$ subintervals, we solved Problem P^r_N for $N = 16, 18, 20, 22, 24$. Our MATLAB program uses the in-built differential equation solver ODE23 to solve the state system (23) and the sensitivity systems (36) and (57).

The optimal objective function values are given in Table 1. Moreover, the optimal control parameters for $N = 24$ are given in Table 2. According to equation (19a), the optimal values in Table 2 are the slopes of the optimal piecewise-linear control, which is

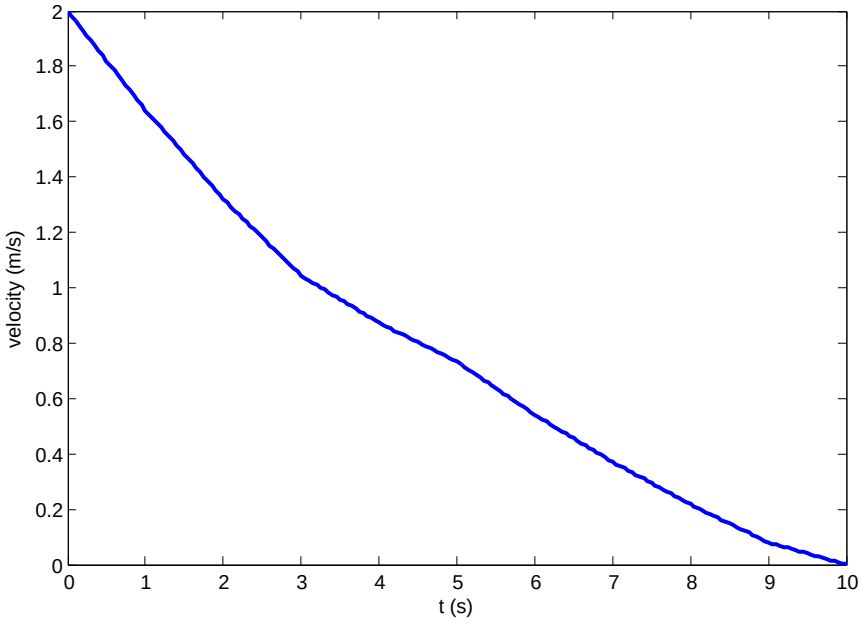

Figure 5: Optimal piecewise-linear control for $N = 24$

Table 1: Optimal objective values for Section 5.1 (piecewise-linear control parameterization)

N	16	18	20	22	24
$J(\sigma)$	64831	60913	37934	29243	25201

plotted in Figure 5. In comparison, the objective values corresponding to the "immediate closure" strategy (in which the valve is closed abruptly) and the "constant closure rate" strategy (in which the valve is closed steadily at a constant rate) are 1.4069×10^{15} and 7.5321×10^{4}, respectively—both much higher than the objective values in Table 1.

5.2. Piecewise-Quadratic Control Parameterization

We set $\alpha = 10^{-6}$ as the smoothing parameter and $\omega = 1$ as the penalty parameter. We observed that ODE23 in MATLAB performs poorly in the piecewise-quadratic case. Thus, we changed the code to use ODE15s instead of ODE23 to solve the state and sensitivity systems. To determine good initial values for $\hat{\sigma}^k$, we constructed an initial piecewise-quadratic function (with smooth derivative) to approximate the optimal piecewise-linear control. This piecewise-quadratic function interpolates the optimal

Table 2: Optimal control parameters for Section 5.1 with $N = 24$ (piecewise-linear control parameterization)

k	1	2	3	4	5
σ^k	-0.3582	-0.3214	-0.2771	-0.1700	-0.1405
k	6	7	8	9	10
σ^k	-0.1923	-0.1702	-0.1533	-0.3750	-0.0795

Table 3: Optimal objective values for Section 5.2 (piecewise-quadratic control parameterization)

N	16	18	20	22	24
$J(\hat{\sigma})$	15262	13911	10192	10190	10187

Table 4: Optimal control parameters for Section 5.2 with $N = 24$ (piecewise-quadratic control parameterization)

k	1	2	3	4	5
$\hat{\sigma}^k$	-0.0577	-0.1220	-0.0096	0.0551	-0.0614
k	6	7	8	9	10
$\hat{\sigma}^k$	-0.0172	-0.0191	-0.0032	-0.0324	0.0943

piecewise-linear control at the temporal knot points, and their derivatives are equal at the initial time. After constructing the initial piecewise-quadratic control, the corresponding initial values of $\hat{\sigma}^k$ were subsequently obtained. The optimal objective function values for $r = 10$ and $N = 16, 18, 20, 22, 24$ are given in Table 3. The optimal control parameters for $N = 24$ are given in Table 4 and the corresponding optimal piecewise-quadratic control is shown in Figure 6. The pressure profiles at the pipeline terminus for the optimal piecewise-quadratic control, the optimal piecewise-linear control, and the constant closure rate control strategy are compared in Figure 7. It is clearly apparent from the figure that the piecewise-quadratic strategy results in the smoothest pressure profile with the least fluctuation. Figure 8 gives another comparison between the different control strategies for the pressure profile along the pipeline at the terminal time $t = 10$s. Moreover, Figures 9-12 show the evolution of the pressure profile over the time and space domains, for each of the four control strategies: immediate closure, constant closure rate, optimal piecewise-linear, and optimal piecewise-quadratic. As expected, the pressure profile for the immediate closure strategy is the most volatile.

6. Conclusions and Future Work

This paper has presented an effective computational method for solving a finite-time optimal control problem for water hammer suppression during valve closure in fluid pipelines. The method is based on a combination of the method of lines (for discretizing the fluid flow PDEs) and the control parameterization method (for discretizing the boundary control function). By applying these two methods in conjunction, the optimal control problem is reduced to an optimal parameter selection problem that can be solved using numerical optimization algorithms. Simulation results demonstrate that this approach is highly effective at mitigating water hammer. Note that our proposed approach involves first discretizing the PDEs to obtain a set of ODEs, and then applying ODE optimal control techniques to determine the optimal valve actuation strategy. An alternative approach would be to apply PDE optimal control techniques directly to the fluid flow model. This will be considered in future work. We also plan to investigate various modifications of the objective function (14). For example, the different terms in

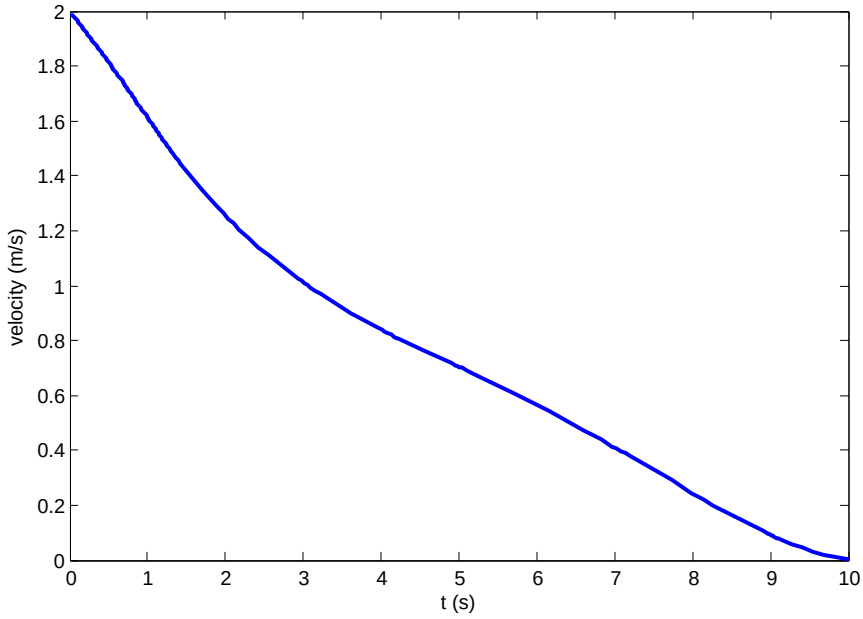

Figure 6: Optimal piecewise-quadratic control for $N = 24$

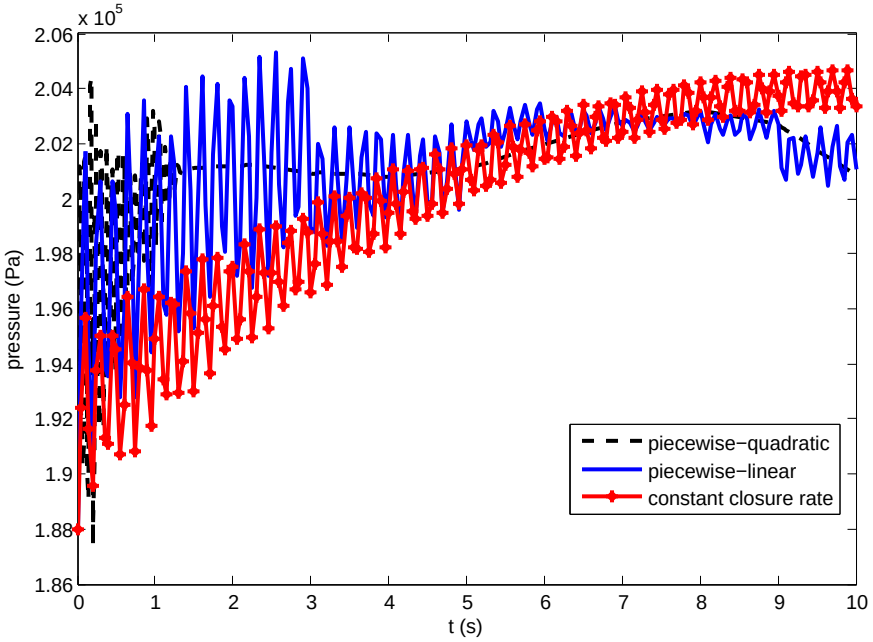

Figure 7: Pressure at the pipeline terminus corresponding to the optimal piecewise-quadratic strategy, the optimal piecewise-linear strategy and the constant closure rate strategy (all for $N = 24$)

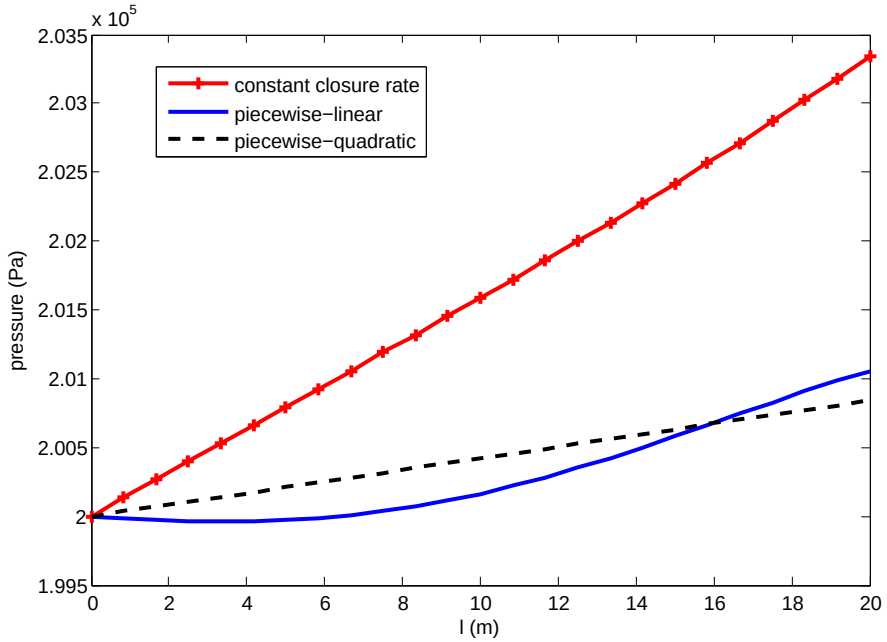

Figure 8: Pressure along the pipeline at the terminal time $t = 10$s corresponding to the optimal piecewise-quadratic strategy, the optimal piecewise-linear strategy and the constant closure rate strategy (all for $N = 24$)

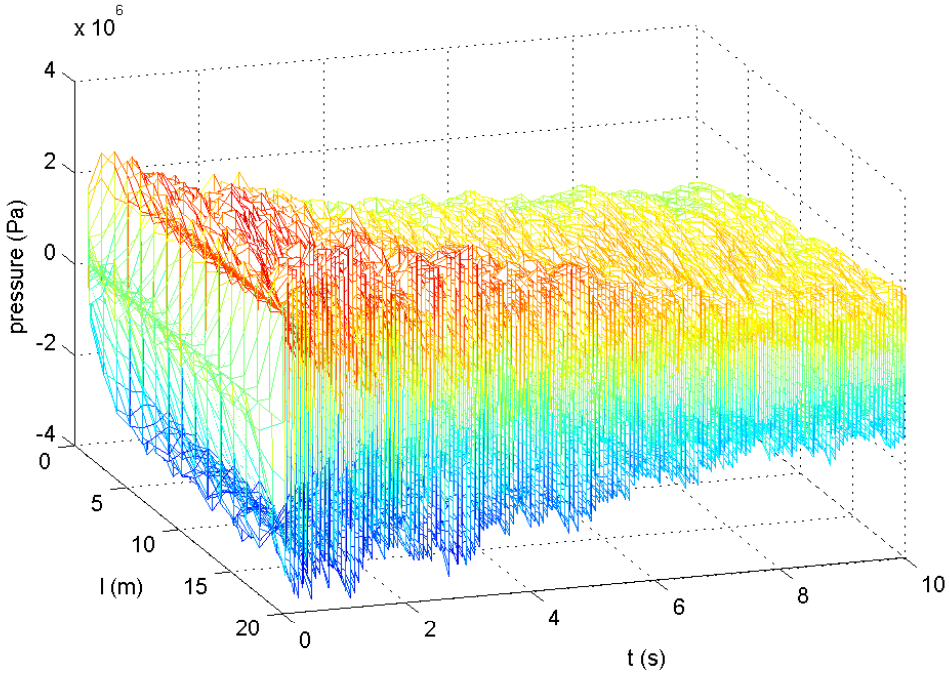

Figure 9: Pressure profile corresponding to the immediate closure strategy

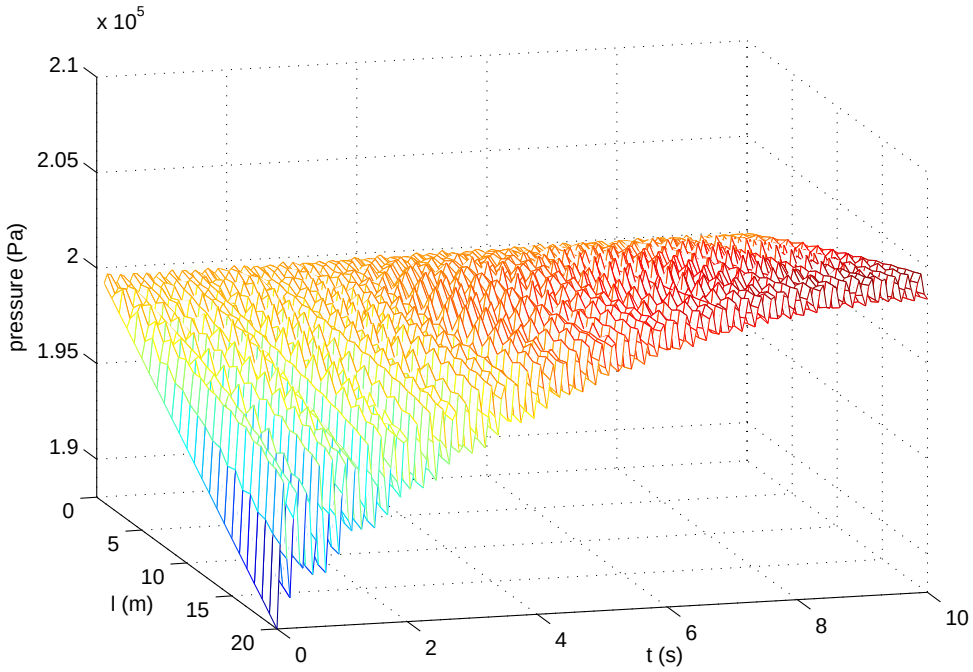

Figure 10: Pressure profile corresponding to the constant closure rate strategy

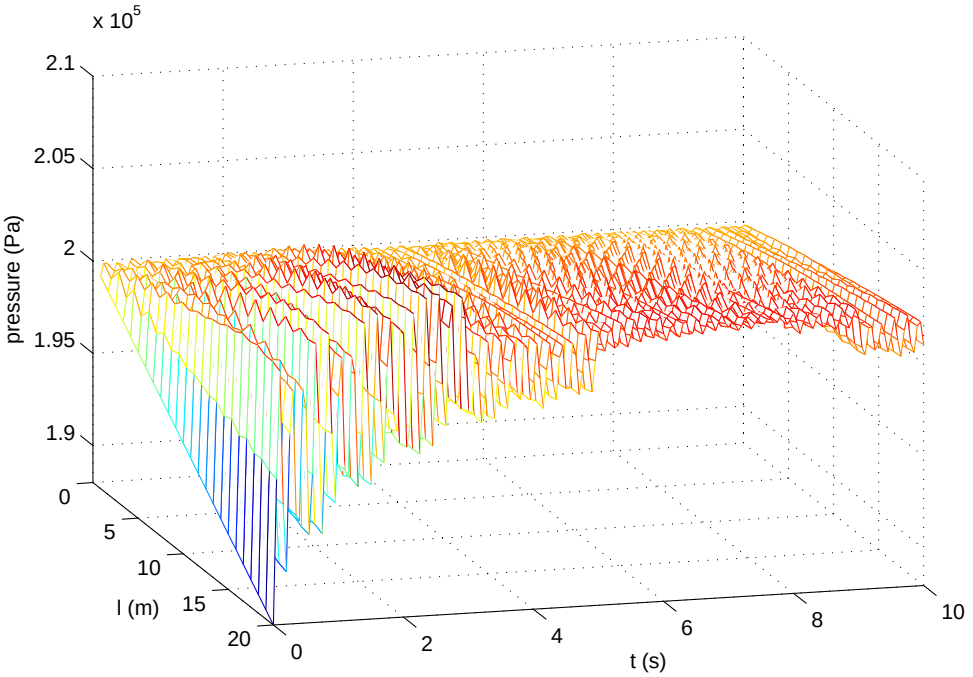

Figure 11: Pressure profile corresponding to the optimal piecewise-linear strategy

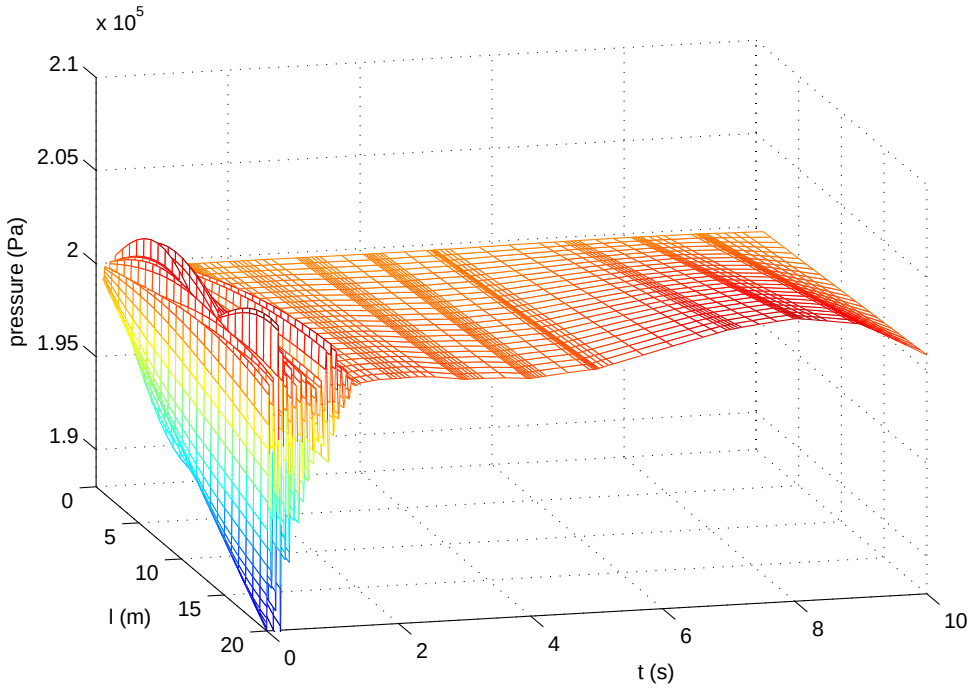

Figure 12: Pressure profile corresponding to the optimal piecewise-quadratic strategy

(14) can be assigned different weights, or the objective can be changed to track a given velocity profile rather than a pressure profile.

References

[1] A. Bergnt, A. R. Simpson, and E. Sijamhodzic. Water hammer analysis of pumping systems for control of water in underground mines. In *Proceedings of the 4th International Mine Water Association Congress*, pages 9–20, 1991.

[2] D. Sciamarella and G. Artana. A water hammer analysis of pressure and flow in the voice production system. *Speech Communication*, 51(4):344–351, 2009.

[3] K. H. Asli, F. B. O. Naghiyev, and A. K. Haghi. Some aspects of physical and numerical modeling of water hammer in pipelines. *Nonlinear Dynamics*, 60(4):677–701, 2010.

[4] W. Erath, B. Nowotny, and J. Maetz. Modelling the fluid structure interaction produced by a water hammer during shutdown of high-pressure pumps. *Nuclear Engineering and Design*, 193(3):283–296, 1999.

[5] C. Schmitt, G. Pluvinage, E. Hadj-Taieb, and R. Akid. Water pipeline failure due to water hammer effects. *Fatigue & Fracture of Engineering Materials & Structures*, 29(12):1075–1082, 2006.

[6] S. Jallouf, C. Schmitt, G. Pluvinage, E. Hadj-Taïeb, and M. Lebienvenu. A probabilistic safety factor for defect assessment of water pipes subjected to water hammer. *The Journal of Strain Analysis for Engineering Design*, 46(1):14–26, 2011.

[7] Y. G. Cai. *Fluid Dynamics in Pipeline Transport.* Zhejiang University Press, Hangzhou, 1990.

[8] M. D. Saikia and A. K. Sarma. Simulation of water hammer flows with unsteady friction factor. *ARPN Journal of Engineering and Applied Sciences*, 1(4):35–40, 2006.

[9] B. Pierre and J. S. Gudmundsson. Coincidental match of numerical simulation and physics. In *IOP Conference Series: Earth and Environment*, 2010.

[10] Y. K. Qiu, B. R. Li, X. Y. Fu, G. Yang, and J. H. Hu. Suppressing water hammer of ship steering systems with hydraulic accumulator. *Proceedings of the Institution of Mechanical Engineers: Part E – Journal of Process Mechanical Engineering*, 228(2):136–148, 2014.

[11] C. S. W. Lavooij and A. S. Tusseling. Fluid-structure interaction in liquid-filled piping systems. *Journal of Fluids and Structures*, 5(5):573–595, 1991.

[12] A. E. Vardy and K. L. Hwang. A characteristics model of transient friction in pipes. *Journal of Hydraulic Research*, 29(5):669–684, 1991.

[13] M. A. Bouaziz, M. A. Guidara, C. Schmitt, E. Hadj-Taïeb, and Z. Azari. Water hammer effects on a gray cast iron water network after adding pumps. *Engineering Failure Analysis*, 44:1–16, 2014.

[14] S. Blažič, G. Geiger, and D. Matko. Application of a heterogenous multiscale method to multi-batch driven pipeline. *Applied Mathematical Modelling*, 38(3):864–877, 2014.

[15] M. Zhao and M. S. Ghidaoui. Godunov-type solutions for water hammer flows. *Journal of Hydraulic Engineering*, 130(4):341–348, 2004.

[16] M. S. Ghidaoui, M. Zhao, D. A. Mcinnis, and D. H. Axworthy. A review of water hammer theory and practice. *Applied Mechanics Reviews*, 58(1):49–76, 2005.

[17] W. E. Schiesser. *The Numerical Method of Lines: Integration of Partial Differential Equations.* Academic Press, Waltham, 1991.

[18] W. E. Schiesser and G. W. Griffiths. *A Compendium of Partial Differential Equation Models: Method of Lines Analysis with Matlab.* Cambridge University Press, Cambridge, 2009.

[19] N. Marian. Model of the water-hammer effect considering a spring safety valve. *Archives of Hydro-Engineering and Environmental Mechanics*, 51(1):25–40, 2004.

[20] B. S. Jung and B. W. Karney. Optimum selection of hydraulic devices for water hammer control in the pipeline systems using genetic algorithm. In *Proceedings of the 4th Joint Fluids Summer Engineering Conference*, pages 2877–2883, 2003.

[21] H. Z. Cao, Z. H. He, and Z. Y. He. The analytic research on the wave process and optimal control of water hammer in pipes. *Engineering Mechanics*, 25(6):22–26, 2008.

[22] D. H. Axworthy and B. W. Karney. Valve closure in graph-theoretical models for slow transient network analysis. *Journal of Hydraulic Engineering*, 126(4):304–309, 2000.

[23] W. X. Tian, G. Su, G. P. Wang, S. Z. Qiu, and Z. J. Xiao. Numerical simulation and optimization on valve-induced water hammer characteristics for parallel pump feedwater system. *Annals of Nuclear Energy*, 35(12):2280–2287, 2008.

[24] W. M. Feng and X. X. Zheng. Research on optimal control of transient multiple valves regulation for fluid transient. *Journal of Wuhan University of Hydraulic and Electric Engineering*, 36(2):130–133, 2003.

[25] E. B. Wylie, V. L. Streeter, and L. Suo. *Fluid Transients in Systems*. Prentice Hall, New Jersey, 1993.

[26] M. S. Ghidaoui. On the fundamental equations of water hammer. *Urban Water Journal*, 1(2):71–83, 2004.

[27] S. Blažič, D. Matko, and G. Geiger. Simple model of a multi-batch driven pipeline. *Mathematics and Computers in Simulation*, 64(6):617–630, 2004.

[28] G. A. Atanov, E. G. Evseeva, and P. A. Work. Variational problem of water-level stabilization in open channels. *Journal of Hydraulic Engineering*, 124(1):50–54, 1998.

[29] Y. Ding and S. S. Wang. Optimal control of open-channel flow using adjoint sensitivity analysis. *Journal of Hydraulic Engineering*, 132(11):1215–1228, 2006.

[30] C. F. Gerald and P. O. Wheatley. *Applied Numerical Analysis*. Pearson, New York, 2003.

[31] K. L. Teo, C. J. Goh, and K. H. Wong. *A Unified Computational Approach to Optimal Control Problems*. Longman Scientific and Technical, Essex, 1991.

[32] Q. Lin, R. C. Loxton, and K. L. Teo. The control parameterization method for nonlinear optimal control: A survey. *Journal of Industrial and Management Optimization*, 10(1):275–309, 2014.

[33] Q. Lin, R. C. Loxton, K. L. Teo, and Y. H. Wu. Optimal control computation for nonlinear systems with state-dependent stopping criteria. *Automatica*, 48(9):2116–2129, 2012.

[34] R. C. Loxton, K. L. Teo, and V. Rehbock. Optimal control problems with multiple characteristic time points in the objective and constraints. *Automatica*, 44(11):2923–2929, 2008.

[35] C. Y. Kaya and J. L. Noakes. Computational method for time-optimal switching control. *Journal of Optimization Theory and Applications*, 117(1):69–92, 2003.

[36] D. G. Luenberger. *Linear and Nonlinear Programming*. Springer, New York, 2003.

[37] R. C. Loxton, K. L. Teo, V. Rehbock, and K. F. C. Yiu. Optimal control problems with a continuous inequality constraint on the state and the control. *Automatica*, 45(10):2250–2257, 2009.

[38] R. C. Loxton, Q. Lin, V. Rehbock, and K. L. Teo. Control parameterization for optimal control problems with continuous inequality constraints: New convergence results. *Numerical Algebra, Control and Optimization*, 2(3):571–599, 2012.

[39] X. G. Liu, Y. Q. Hu, J. H. Feng, and K. Liu. A novel penalty approach for nonlinear dynamic optimization problems with inequality path constraints. *IEEE Transactions on Automatic Control*, Accepted, 2014.

[40] X. Zhao, X. Y. Zhang, M. D. Zhao, and H. Y. Dong. *Hydraulics*. China Electric Power Press, Beijing, 2009.

[41] D. F. Yan. *Design and Management of Oil Pipeline*. Petroleum Industry Press, Beijing, 1986.